CHEMISTRY
AN ASIAN JOURNAL

Supporting Information

Anticancer Potencies of Pt^{II}- and Pd^{II}-linked M_2L_4 Coordination Capsules with Improved Selectivity

Anife Ahmedova,*[a] Denitsa Momekova,[b] Masahiro Yamashina,[c] Pavletta Shestakova,[d] Georgi Momekov,[b] Munetaka Akita,[c] and Michito Yoshizawa*[c]

asia_201501238_sm_miscellaneous_information.pdf

Contents

Materials and methods

NMR: Bruker AVANCE-400 (400 MHz), ASCEND-500 (500 MHz) or Bruker AVANCE II+ 600 MHz.

ESI-TOF MS: Bruker micrOTOF II.

Fluorescence microscopy: Optika N400-FL microscope equipped with 40X objective and CCD camera.

Solvents and reagents: TCI Co., Ltd., Wako Pure Chemical Industries Ltd., Kanto Chemical Co., Inc., Sigma-Aldrich Co., and Cambridge Isotope Laboratories, Inc.

Compounds: Ligand **2** and capsules $\mathbf{1}^{\mathbf{Pt}}$ and $\mathbf{1}^{\mathbf{Pd}}$ were synthesized following procedures described previously.[1,2]

Synthesis of $\mathbf{1}^{\mathbf{Pt}}\bullet(\mathrm{Pyr})_2$ and $\mathbf{1}^{\mathbf{Pd}}\bullet(\mathrm{Pyr})_2$ composites

A 1:2 host-guest composite, $\mathbf{1}^{\mathbf{Pt}}\bullet(\mathrm{Pyr})_2$, was synthesized from Pt(II) capsule $\mathbf{1}^{\mathbf{Pt}}$ and pyrene (Pyr) according to the previously reported procedure.[3] A $\mathbf{1}^{\mathbf{Pd}}\bullet(\mathrm{Pyr})_2$ composite was also prepared by the similar procedure.

Physical data of $\mathbf{1}^{\mathbf{Pt}}\bullet(\mathrm{Pyr})_2$: ^{1}H NMR (500 MHz, D_2O:CD_3OD = 1:2, r.t.): δ3.14 (m, 28H, $\mathbf{1}^{\mathbf{Pt}}$ and Pyr), 3.62-3.78 (m, 24H, $\mathbf{1}^{\mathbf{Pt}}$ and Pyr), 3.99 (s, 12H, $\mathbf{1}^{\mathbf{Pt}}$), 4.03 (d, J = 9.0 Hz, 4H, Pyr), 4.45 (m, 8H, $\mathbf{1}^{\mathbf{Pt}}$), 4.56-4.73 (m, 20H, $\mathbf{1}^{\mathbf{Pt}}$ and Pyr), 5.06 (m, 8H, $\mathbf{1}^{\mathbf{Pt}}$), 5.60 (s, 8H, $\mathbf{1}^{\mathbf{Pt}}$), 6.75 (d, J = 8.5 Hz, 8H, $\mathbf{1}^{\mathbf{Pt}}$), 6.97 (s, 4H, $\mathbf{1}^{\mathbf{Pt}}$), 7.23 (d, J = 8.5 Hz, 8H, $\mathbf{1}^{\mathbf{Pt}}$), 7.71 (dd, J = 8.5, 7.5 Hz, 8H, $\mathbf{1}^{\mathbf{Pt}}$), 7.89 (dd, J = 8.5, 7.5 Hz, 8H, $\mathbf{1}^{\mathbf{Pt}}$), 8.27-8.35 (m, 16H, $\mathbf{1}^{\mathbf{Pt}}$), 8.44 (dd, J = 8.0, 5.5 Hz, 8H, $\mathbf{1}^{\mathbf{Pt}}$), 8.50 (d, J = 8.5 Hz, 8H, $\mathbf{1}^{\mathbf{Pt}}$), 8.63 (d, J = 8.5 Hz, 8H, $\mathbf{1}^{\mathbf{Pt}}$), 8.73 (d, J = 5.5 Hz, 8H, $\mathbf{1}^{\mathbf{Pt}}$), 8.87 (d, J = 8.0 Hz, 8H, $\mathbf{1}^{\mathbf{Pt}}$). ESI-TOF MS (H_2O:CH_3OH): m/z 2072.3 $[\mathbf{1}^{\mathbf{Pt}}\bullet(\mathrm{Pyr})_2 - 2\bullet NO_3^-]^{2+}$, 1360.9 $[\mathbf{1}^{\mathbf{Pt}}\bullet(\mathrm{Pyr})_2 - 3\bullet NO_3^-]^{3+}$, 1005.2 $[\mathbf{1}^{\mathbf{Pt}}\bullet(\mathrm{Pyr})_2 - 4\bullet NO_3^-]^{4+}$.

Physical data of $\mathbf{1}^{\mathbf{Pd}}\bullet(\mathrm{Pyr})_2$: ^{1}H NMR (500 MHz, D_2O:CD_3OD = 1:2, r.t.): δ3.13 (s, 24H, $\mathbf{1}^{\mathbf{Pd}}$), 3.18 (d, J = 7.5 Hz, 4H, Pyr), 3.60-3.81 (m, 24H, $\mathbf{1}^{\mathbf{Pd}}$ and Pyr), 3.99 (s, 12H, $\mathbf{1}^{\mathbf{Pd}}$), 4.06 (d, J = 8.5 Hz, 4H, Pyr), 4.49 (m, 8H, $\mathbf{1}^{\mathbf{Pd}}$), 4.58-4.71 (m, 20H, $\mathbf{1}^{\mathbf{Pd}}$ and Pyr), 5.05 (m, 8H, $\mathbf{1}^{\mathbf{Pd}}$), 5.55 (s, 8H, $\mathbf{1}^{\mathbf{Pd}}$), 6.69 (d, J = 8.5 Hz, 8H, $\mathbf{1}^{\mathbf{Pd}}$), 6.99 (s, 4H, $\mathbf{1}^{\mathbf{Pd}}$), 7.22 (d, J = 8.5 Hz, 8H, $\mathbf{1}^{\mathbf{Pd}}$), 7.68 (dd, J = 8.5, 7.5 Hz, 8H, $\mathbf{1}^{\mathbf{Pd}}$), 7.88 (dd, J = 8.5, 7.5 Hz, 8H, $\mathbf{1}^{\mathbf{Pd}}$), 8.25-8.34 (m, 16H, $\mathbf{1}^{\mathbf{Pd}}$), 8.43 (dd, J = 8.0, 5.5 Hz, 8H, $\mathbf{1}^{\mathbf{Pd}}$), 8.50 (d, J = 8.5 Hz, 8H, $\mathbf{1}^{\mathbf{Pd}}$), 8.62 (d, J = 8.5 Hz, 8H, $\mathbf{1}^{\mathbf{Pd}}$), 8.67 (d, J = 5.5 Hz, 8H, $\mathbf{1}^{\mathbf{Pd}}$), 8.83 (d, J = 8.0 Hz, 8H, $\mathbf{1}^{\mathbf{Pd}}$). ESI-TOF MS (H_2O:CH_3OH = 1:2): m/z 1983.8 $[\mathbf{1}^{\mathbf{Pd}}\bullet(\mathrm{Pyr})_2 - 2\bullet NO_3^-]^{2+}$, 1302.2 $[\mathbf{1}^{\mathbf{Pd}}\bullet(\mathrm{Pyr})_2 - 3\bullet NO_3^-]^{3+}$, 961.2 $[\mathbf{1}^{\mathbf{Pd}}\bullet(\mathrm{Pyr})_2 - 4\bullet NO_3^-]^{4+}$.

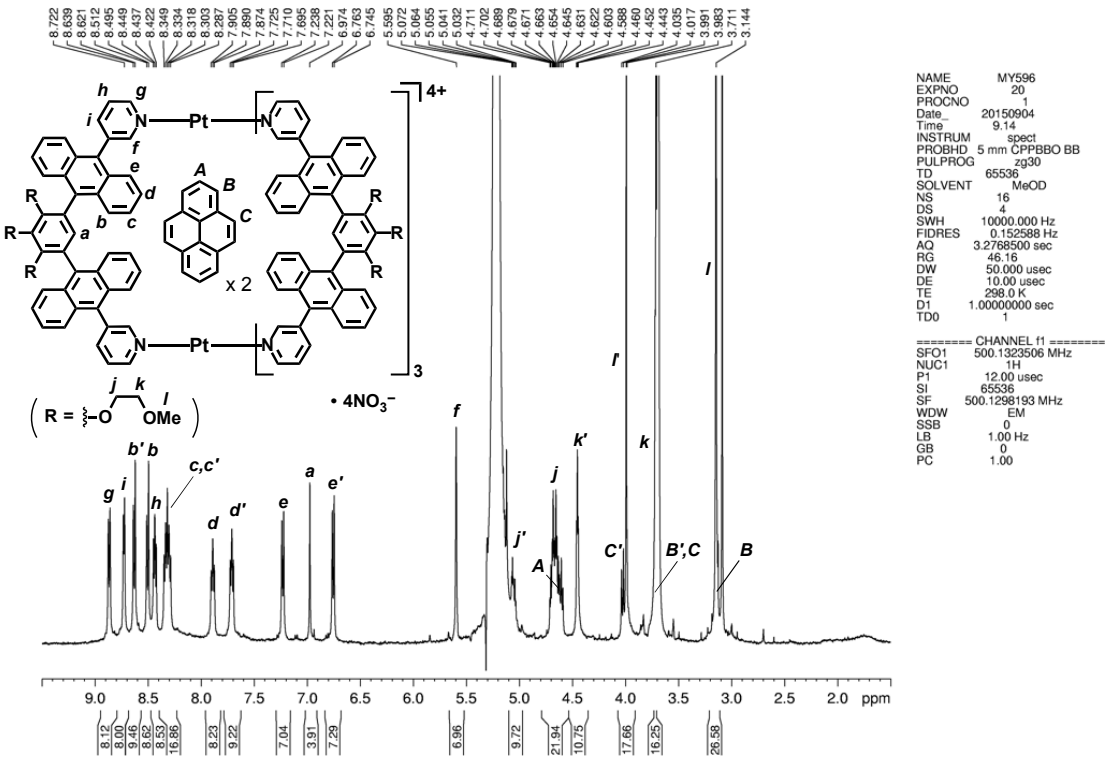

Figure S1a. ^{1}H NMR spectrum (500 MHz, D_2O:CD_3OD = 1:2, r.t.) of $\mathbf{1}^{\mathbf{Pt}}\bullet(Pyr)_2$.

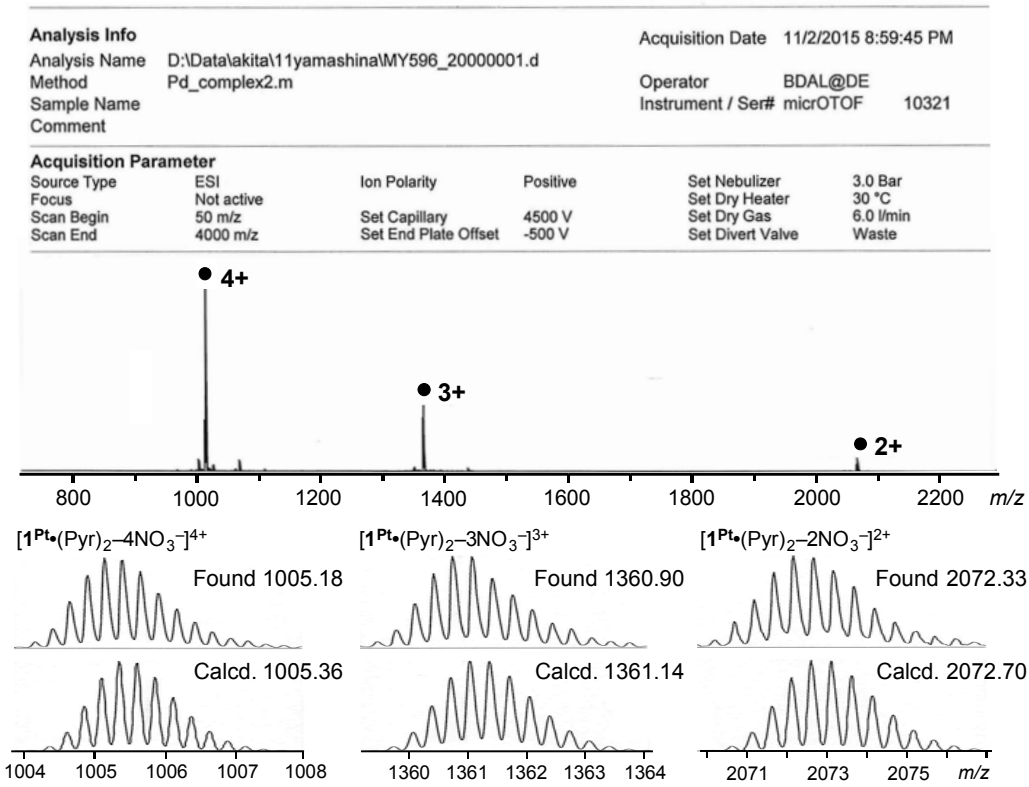

Figure S1b. ESI-TOF MS spectrum (H_2O:CH_3OH = 1:2) of $\mathbf{1}^{\mathbf{Pt}}\bullet(Pyr)_2$.

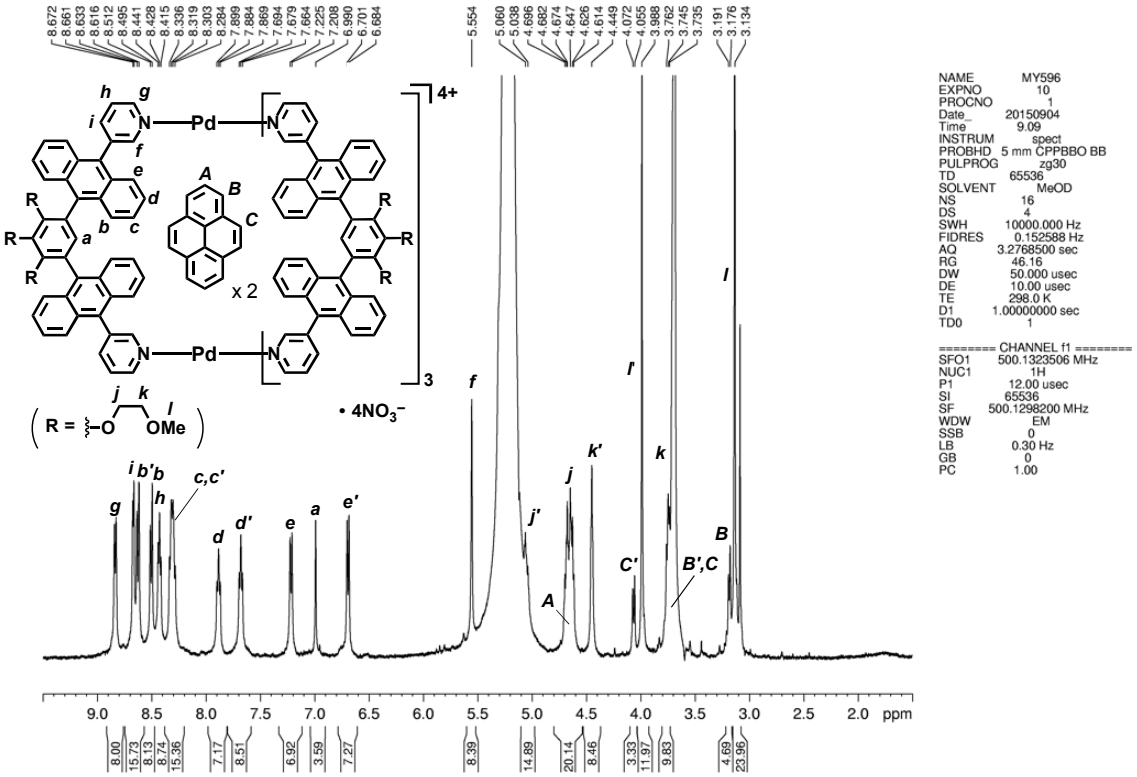

Figure S2a. ^{1}H NMR spectrum (500 MHz, D_2O:CD_3OD = 1:2, r.t.) of $\mathbf{1}^{Pd}\bullet(Pyr)_2$.

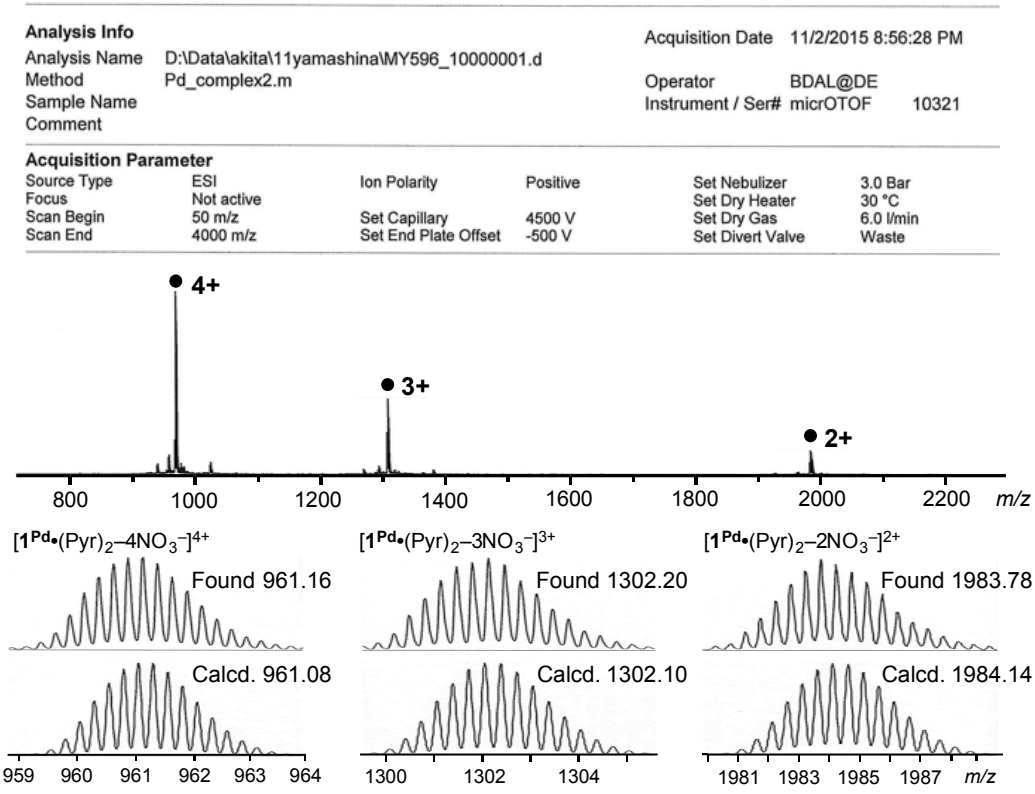

Figure S2b. ESI-TOF MS spectrum (H_2O:CH_3OH = 1:2) of $\mathbf{1}^{Pd}\bullet(Pyr)_2$.

Stability of capsules 1^{Pt} and 1^{Pd} toward biomolecules

Stability of capsules $\mathbf{1}^{Pt}$ and $\mathbf{1}^{Pd}$ in presence of various biomolecules (shown in Figure 2) was studied by mixing the substances in D_2O:CD_3OD (3:2) solutions in molar ratios of capsule:biomolecule from 1:2 to 1:100. The resultant solutions were stirred at 50 ºC (or room temperature) and monitored by ^{1}H NMR spectroscopy in the course of 1 to 3 days. The interaction of the capsules with glutathione was additionally studied in a DMSO-d_6:D_2O (10:1) solution in order to avoid an eventual precipitation.

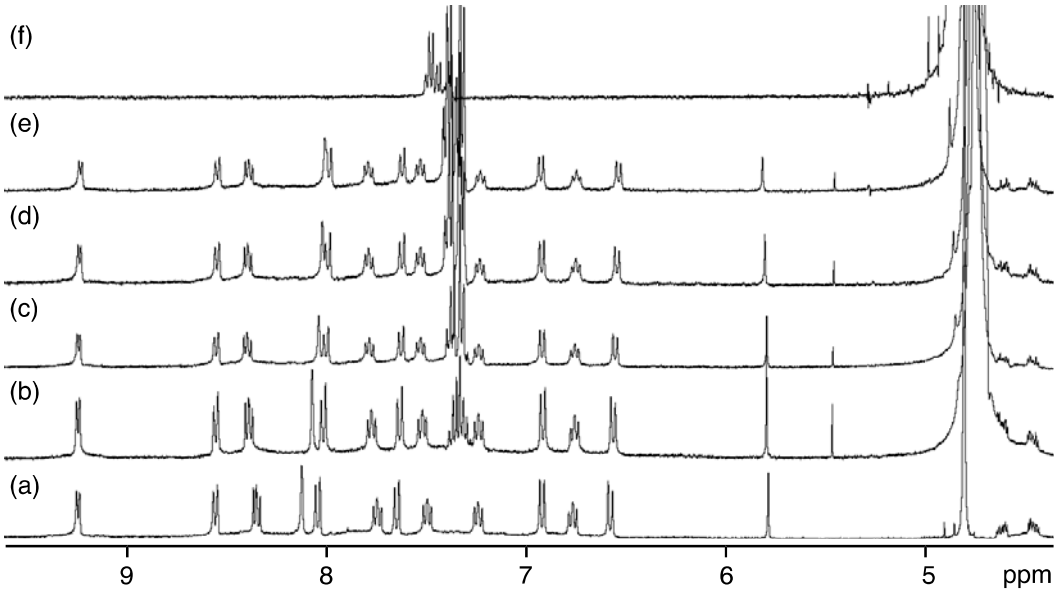

Figure S3. ^{1}H NMR spectra (400 MHz, D_2O:CD_3OD = 3:2, r.t.) of a) $\mathbf{1}^{Pt}$, b) $\mathbf{1}^{Pt}$ + phenylalanine (1 equiv.), c) $\mathbf{1}^{Pt}$ + phenylalanine (2 equiv.), d) $\mathbf{1}^{Pt}$ + phenylalanine (4 equiv.), and e) $\mathbf{1}^{Pt}$ + phenylalanine (6 equiv.), and f) phenylalanine (in D_2O).

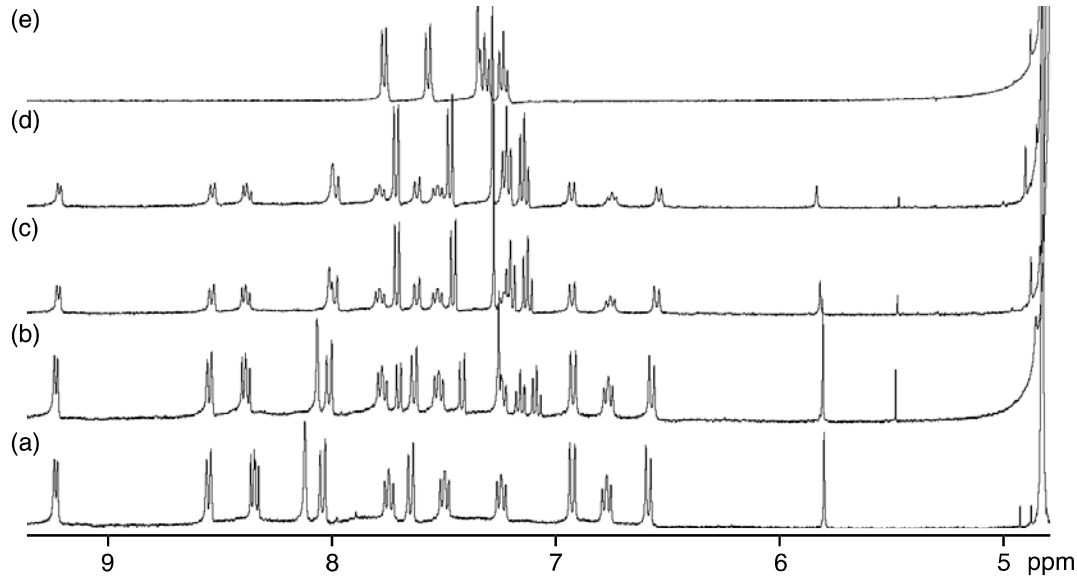

Figure S4. ^{1}H NMR spectra (400 MHz, D_2O:CD_3OD = 3:2, r.t.) of a) $\mathbf{1}^{Pt}$, b) $\mathbf{1}^{Pt}$ + tryptophan (1 equiv.), c) $\mathbf{1}^{Pt}$ + tryptophan (4 equiv.), d) $\mathbf{1}^{Pt}$ + tryptophan (6 equiv.), and e) tryptophan (in D_2O).

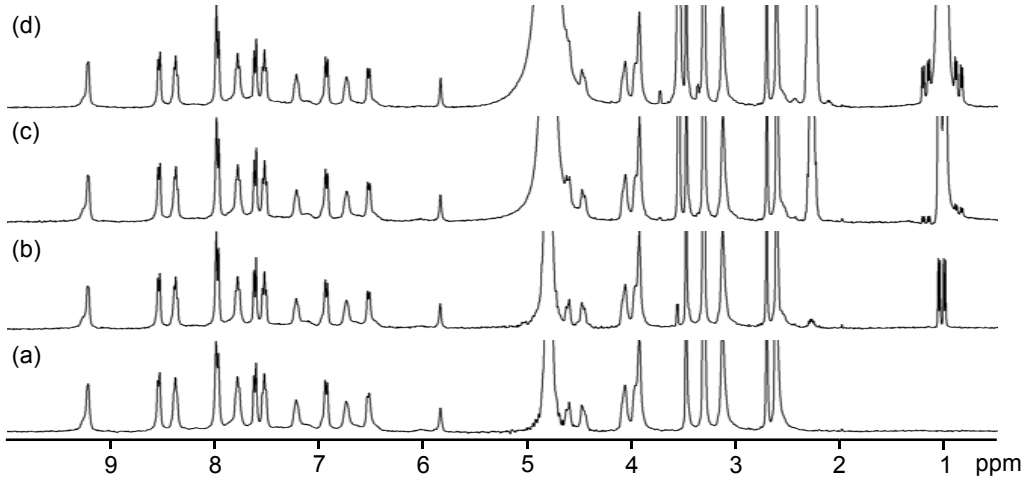

Figure S5a. ^{1}H NMR spectra (400 MHz, D_2O:CD_3OD = 3:2, r.t.) of a) $\mathbf{1}^{Pt}$, b) $\mathbf{1}^{Pt}$ + valine (1 equiv.), c) $\mathbf{1}^{Pt}$ + valine (10 equiv.), and d) $\mathbf{1}^{Pt}$ + valine (100 equiv.).

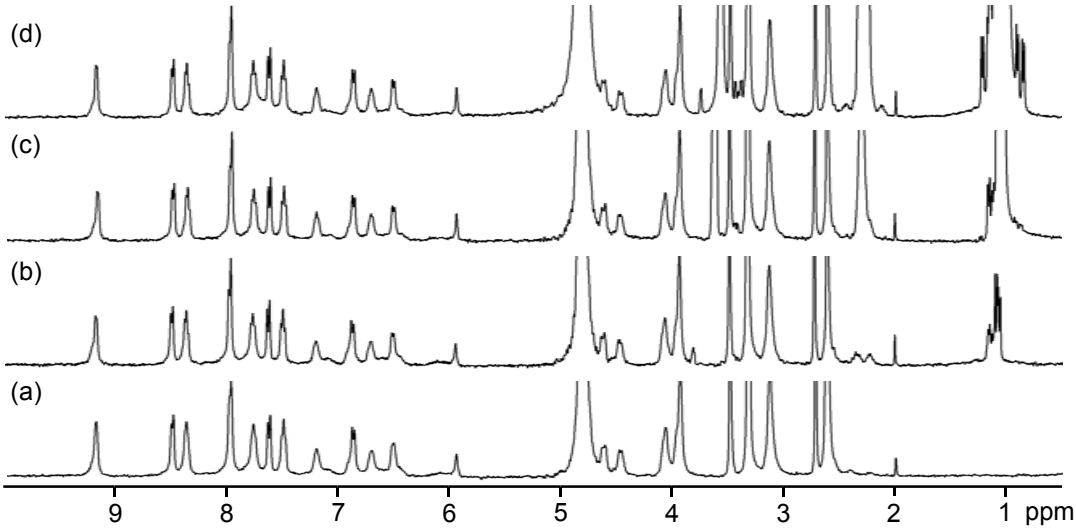

Figure S5b. ^{1}H NMR spectra (400 MHz, D_2O:CD_3OD = 3:2, r.t.) of a) $\mathbf{1}^{Pd}$, b) $\mathbf{1}^{Pd}$ + valine (1 equiv.), c) $\mathbf{1}^{Pd}$ + valine (10 equiv.), and d) $\mathbf{1}^{Pd}$ + valine (100 equiv.).

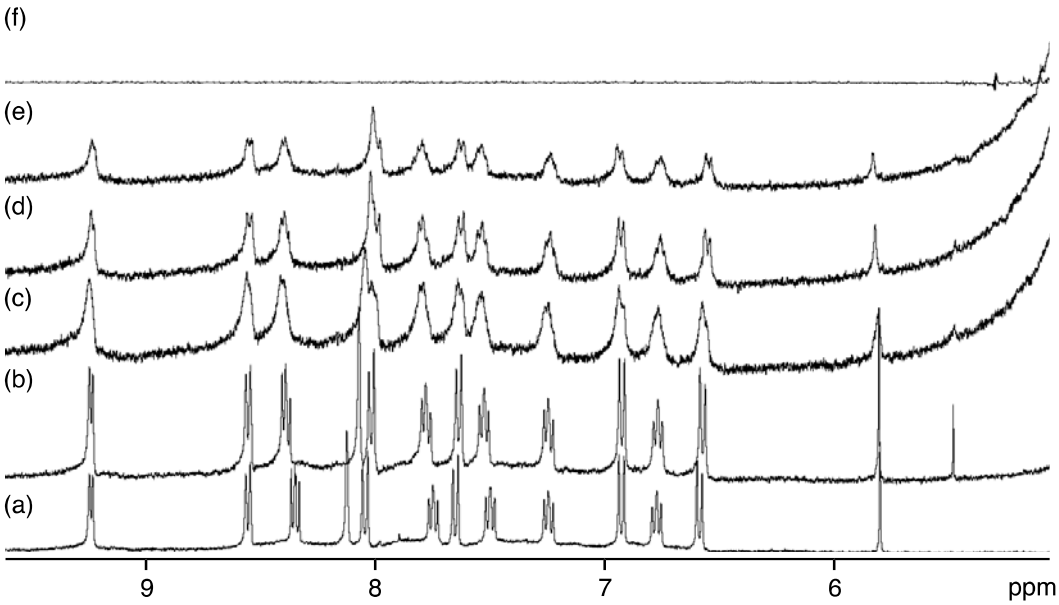

Figure S6a. ^{1}H NMR spectra (400 MHz, D_2O:CD_3OD = 3:2, r.t.) of a) $\mathbf{1}^{Pt}$, b) $\mathbf{1}^{Pt}$ + proline (1 equiv.), c) $\mathbf{1}^{Pt}$ + proline (2 equiv.), d) $\mathbf{1}^{Pt}$ + proline (4 equiv.), e) $\mathbf{1}^{Pt}$ + proline (6 equiv.), and f) proline (in D_2O).

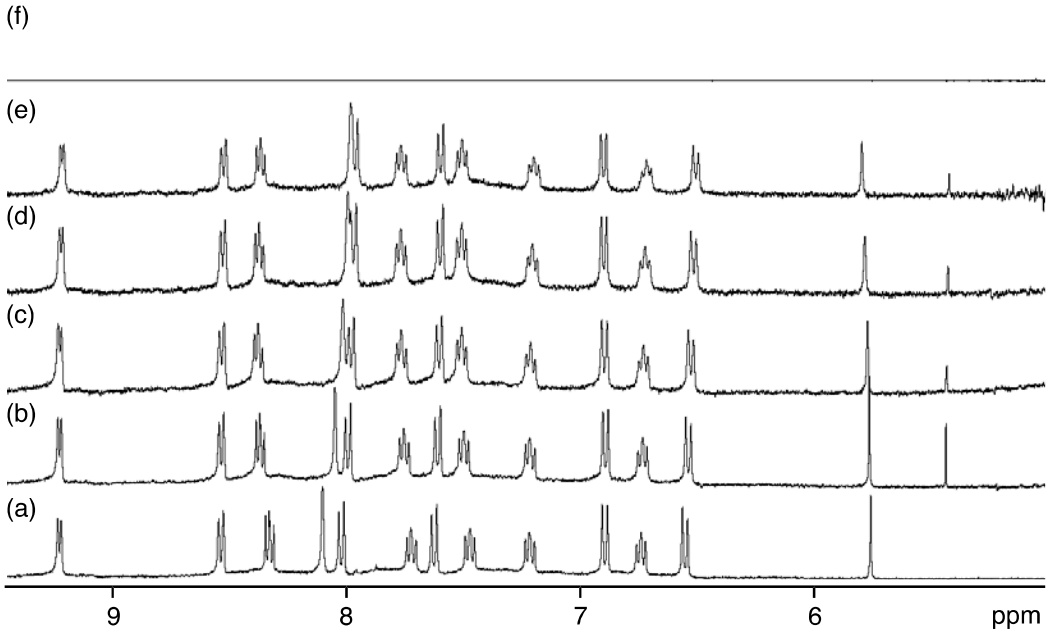

Figure S7a. ^{1}H NMR spectra (400 MHz, D_2O:CD_3OD = 3:2, r.t.) of a) $\mathbf{1}^{Pt}$, b) $\mathbf{1}^{Pt}$ + cysteine (1 equiv.), c) $\mathbf{1}^{Pt}$ + cysteine (2 equiv.), d) $\mathbf{1}^{Pt}$ + cysteine (4 equiv.), e) $\mathbf{1}^{Pt}$ + cysteine (6 equiv.), and f) cysteine (in D_2O).

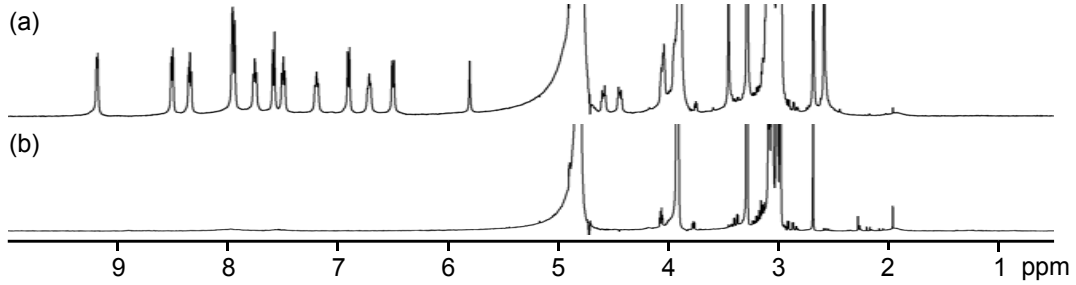

Figure S7b. ^{1}H NMR spectra (500 MHz, D_2O:CD_3OD = 3:2, r.t.) of a) $\mathbf{1}^{Pt}$ + cysteine (~100 equiv.) and b) $\mathbf{1}^{Pd}$ + cysteine (~100 equiv.).

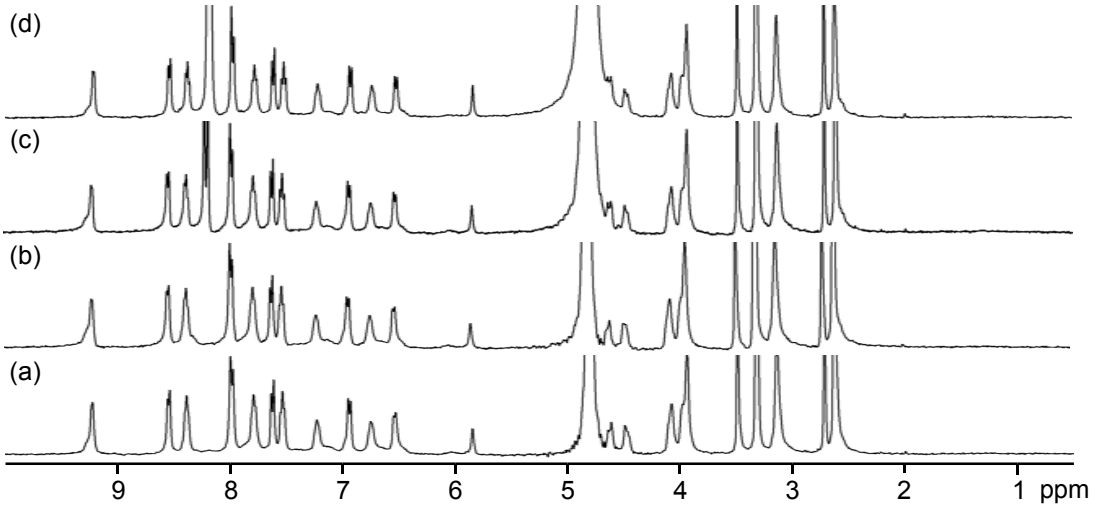

Figure S8a. ^{1}H NMR spectra (400 MHz, D_2O:CD_3OD = 3:2, r.t.) of a) $\mathbf{1}^{\mathbf{Pt}}$, b) $\mathbf{1}^{\mathbf{Pt}}$ + adenine (1 equiv.), c) $\mathbf{1}^{\mathbf{Pt}}$ + adenine (10 equiv.), and d) $\mathbf{1}^{\mathbf{Pt}}$ + adenine (100 equiv.).

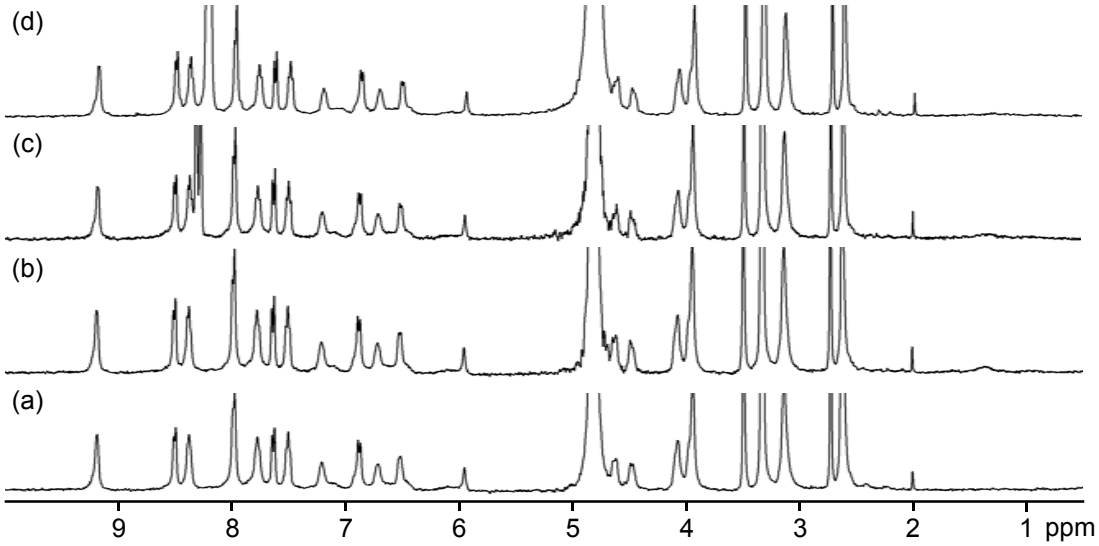

Figure S8b. ^{1}H NMR spectra (400 MHz, D_2O:CD_3OD = 3:2, r.t.) of a) $\mathbf{1}^{\mathbf{Pd}}$, b) $\mathbf{1}^{\mathbf{Pd}}$ + adenine (1 equiv.), c) $\mathbf{1}^{\mathbf{Pd}}$ + adenine (10 equiv.), and d) $\mathbf{1}^{\mathbf{Pd}}$ + adenine (100 equiv.).

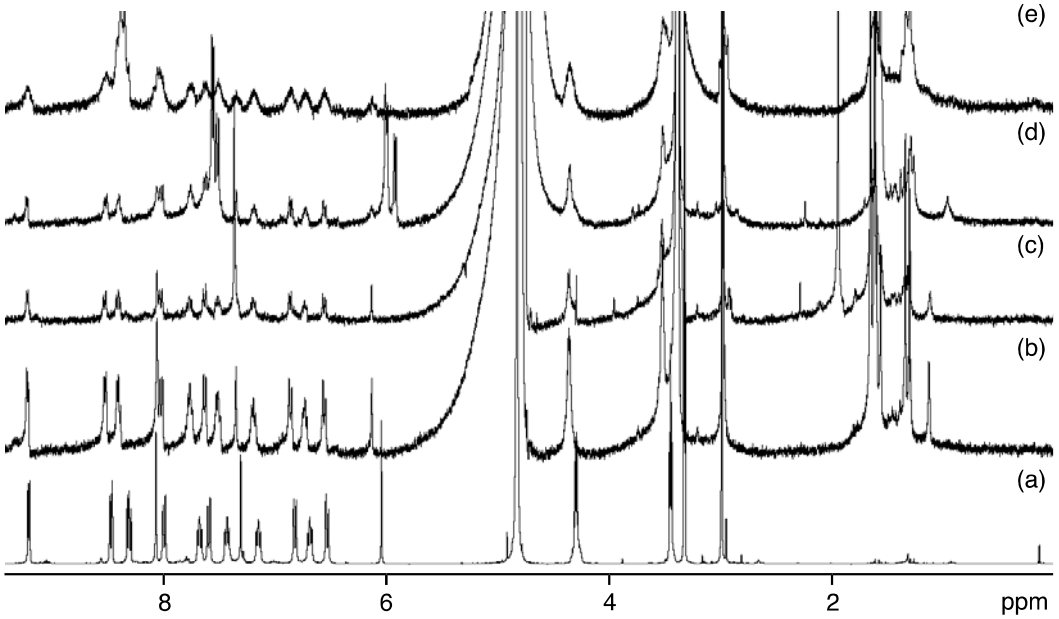

Figure S9. ^{1}H NMR spectra (400 MHz, D_2O:CD_3OD = 3:2, r.t.) of a) **1'^{Pd}**, b) **1'^{Pd}** + adenine, c) **1'^{Pd}** + cytosine, d) **1'^{Pd}** + thymine, and e) **1'^{Pd}** + guanine (**1'^{Pd}** is an analogue of **1^{Pd}**).

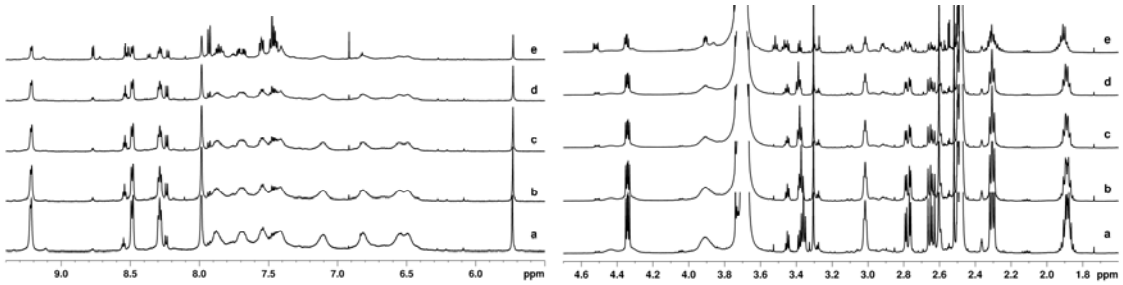

Figure S10. ^{1}H NMR spectra (600 MHz, DMSO-d_6:D_2O = 10:1, r.t.) of **1^{Pt}** + glutathione (10 equiv.) measured immediately after mixing (a) and after b) 1h 30 min, c) 4h 30 min, d) 7h 30 min, and e) 3 days in air.

Cancer cell growth inhibitory evaluation

Cell lines and culture conditions: The pharmacological study was carried out using human tumor cell lines, namely HL-60 (acute myelocyte leukemia), its cisplatin-resistant sub-line HL-60/CDDP, and SKW-3 (T-cell leukemia), as well as a human embryonic kidney cell line HEK-293, utilized as an *in vitro* model for nephrotoxicity. The cisplatin-resistant sub-line HL-60/CDDP has been developed at the Lab of Experimental Chemotherapy (Faculty of Pharmacy, MU-Sofia). It was established by continuous selection in medium with gradually increasing concentrations of cisplatin. HL-60 were obtained from the German Collection of Microorganisms and Cell Cultures (DSMZ GmbH, Braunschweig, Germany). The cells were cultured in a controlled environment – cell culture flasks at 37 °C in an incubator 'BB 16-Function Line' Heraeus (Kendro, Hanau, Germany) with humidified atmosphere and 5% CO_2. The growth medium was 90% RPMI-1640 + 10% FBS. HL-60/CDDP cells were grown in the presence of 25 μmol/L cisplatin in order to maintain their drug resistance phenotype.

MTT-dye reduction assay: The tumor cell growth inhibitory effects of the tested compounds were evaluated using the MTT-dye reduction assay, as previously described,[4] with slight modifications.[5] In brief, exponentially proliferating cells were seeded in 96-well flat-bottomed microplates (100 μL/well; at a density of 1×10^5 cells/mL for the leukemic cells) and incubated for 24 h at 37 °C, in an incubator. Thereafter the cells were exposed to serial dilutions of the tested compounds for 72 h. For each treatment-group a set of at least 8 wells was used. After the exposure period 10 μL aliquots of MTT solution (10 mg/mL in PBS) were pipetted in each well. Thereafter the microplates were incubated for further 4 h at 37 °C and the MTT-formazan crystals formed were dissolved through addition of 100 μL/well 5% formic acid solution in 2-propanol. The MTT-formazan absorption was determined using a multimode microplate reader (Beckman Coulter DTX-880) at 580 nm. The bioassay data were normalized as percentage of the untreated control (set as 100% viable) and fitted to sigmoidal dose response curves allowing the determination of the equieffective IC_{50} concentrations (concentrations inducing 50% suppression of cellular viability). In addition, the resistance indices as a relative merit for the level of resistance in HL-60/CDDP were determined as the ratio between the IC_{50} in the multi-drug resistant

HL-60/CDDP and the corresponding IC_{50} in the sensitive parent line HL-60. All tests were run in triplicate.

In vitro nephrotoxicity and selectivity study

In order to identify the anticancer selectivity of $\mathbf{1}^{Pt}$, $\mathbf{1}^{Pd}$ and cisplatin the inhibitory effects of these agent in HEK-293, where compared to those in the cancer cell lines. To meet this objective the selectivity indices were calculated as a ratio between the IC_{50} obtained in HEK-293 and the arithmetic mean of the IC_{50} values established in the malignant cell lines (in case of cisplatin the value in HL-60/CDDP was ignored as this cell line is not-responsive to this drug).

Table S1. Estimated IC_{50} values of capsules $\mathbf{1}^{Pt}$ and $\mathbf{1}^{Pd}$, cisplatin, and ligand **2** against HL-60, HL-60/CDDP, SKW-3, and HEK-293 cell lines.

compound	IC_{50} (μM)			
	HL-60	HL-60/CDDP (RI)[a]	SKW-3	HEK-293
$\mathbf{1}^{Pt}$	6.6 ± 0.9	1.7 ± 0.3 (0.26)	2.3 ± 0.8	26.4 ± 3.1
$\mathbf{1}^{Pd}$	1.9 ± 0.2	1.0 ± 0.04 (0.51)	1.8 ± 0.2	18.3 ± 1.2
cisplatin	8.1 ± 1.4	124.4 ± 11.7 (15.4)	9.3 ± 2.1	19.3 ± 2.2
ligand **2**	> 100	n.d.	> 80	n.d.

[a]Resistance index (RI) = $IC_{50}^{(HL\text{-}60/CDDP)}/IC_{50}^{(HL\text{-}60)}$. n.d. - Not determined

Fluorescence microscopy imaging study

We made fluorescence microscopy imaging of the HL-60 cells after treating them with ligand **2** and capsules $\mathbf{1}^{M}$ (M = Pd and Pt) (10 μM each) for 4 h (Figure S11). The cells were washed before fixing and imaging. The supernatant of the cells was used to measure the LDH-activity in a kinetic mode and using LDH Assay kit. As LDH (lactate dehydrogenase) is an enzyme that has higher concentration inside the cell, an eventually increased activity of this enzyme in the supernatant would suggest damage of the cells membrane. Our results showed that in all four cases (3 compounds + control) the LDH activity is comparable (ranging from 84-120 U/L with the highest activity in the control). These results suggested that the compounds do not destroy the cell membranes for at

least 4 h. In the Figure 11c, the observed, strong blue fluorescence inside the cells are derived from the decomposition of the non-fluorescent Pd(II) capsule, because the free ligand provides strong fluorescent properties (Figure 11b). At the same time the supernatant of the cells treated with the capsules exhibit negligible (for Pd capsule) or no fluorescence emission (for Pt capsule) in contrast to the supernatant of cells treated with the free ligand **2**.

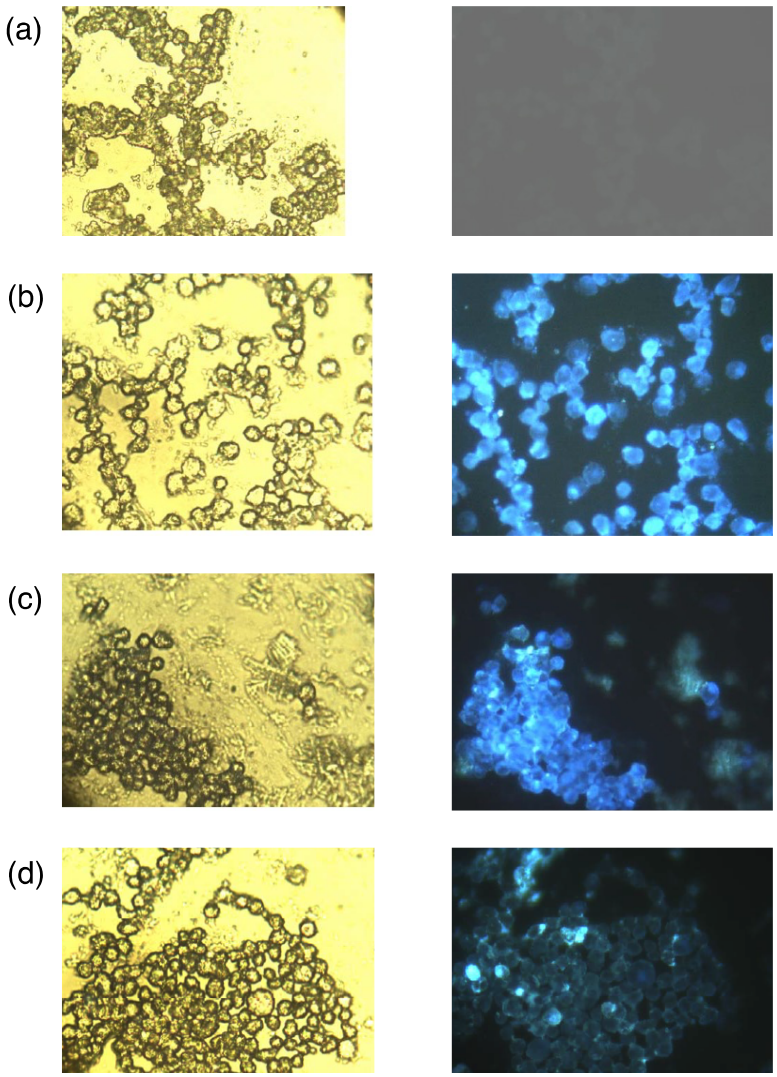

Figure S11. Fluorescence microscopy images (left: transmitted light and right: fluorescent light) of a) HL-60 cells (control) and HL-60 cells treated with: b) ligand **2**, c) $\mathbf{1}^{\mathbf{Pd}}$ capsule, and d) $\mathbf{1}^{\mathbf{Pt}}$ capsule for 4 hours with concentrations of 10 μM.

References

[1] N. Kishi, M. Akita, M. Kamiya, S. Hayashi, H.-F. Hsu, M. Yoshizawa, *J. Am. Chem. Soc.*, **2013**, *135*, 12976–12979.

[2] M. Yamashina, Y. Sei, M. Akita, M. Yoshizawa, *Nat. Commun.,* **2014**, *5*, 4662.

[3] Z. Li, N. Kishi, K. Yoza, M. Akita, M. Yoshizawa, *Chem. Eur. J.,* **2012**, *18*, 8358–8365.

[4] T. Mosmann, *J. Immunol. Methods*, **1983**, *65*, 55–63.

[5] S. M. Konstantinov, H. Eibl, M. R. Berger, *Br. J. Haematol.*, **1999**, *107*, 365–380.